Real-Time Control of Atomic Motion Using Feedback

J. L. Hanssen, V. Milner, T. P. Meyrath, and M. G. Raizen

Center for Nonlinear Dynamics and Department of Physics, The University of Texas at Austin, Austin, Texas 78712-1081

raizen@physics.utexas.edu

Abstract: We demonstrate real-time feedback control of atomic center of mass motion in a cloud of laser cooled cesium atoms. Using the velocity measurement technique of recoil-induced resonances, the average velocity of the atomic cloud is obtained. This information is used to give a correction from a moving optical lattice. We are able to bring the cloud of atoms to a stop with a controllable amount of heating.

OCIS codes: (020.0020) Atomic and molecular physics; (070.4560) Optical data processing

1 Introduction

Manipulating ensembles of particles with feedback has evolved significantly since its use to increase the luminosity of antiproton beams [1]. This has led to proposals for cooling neutral atoms [2] and ions [3], as well as manipulation of wavepackets with ultrafast laser pulses [4]. The basic idea for feedback control of a physical system involves several steps. First, a measurement is made which probes the state of the system. Second, a correction to the system state is performed based on the result of the measurement. These together constitute feedback which may be used to control the system. The measurement as well as correction method vary among the various proposals and experiments in the field. In an experiment where the state of a system is to be controlled, it is desirable for the measurement to be as nondestructive as possible. Some experimental work [5] has involved the use of a high finesse optical cavity to monitor the position of an atom in real-time and to trigger on a far-off-resonance dipole force trap (FORT) to confine the atom to a cavity mode. Other recent work [6] has involved making position measurements of atoms in an optical lattice and feedback to alter the oscillations of the atoms within the lattice. In this demonstration of real-time feedback control, we use the method of recoil-induced resonances (RIR) [7, 8] to make a center-of-mass momentum measurement of a cloud of atoms and a moving optical lattice for changing the state of the system.

This experimental demonstration of real-time feedback control is a simplified single iteration model of stochastic cooling as discussed in Ref. [2]. A stochastic cooling setup entails a measurement and feedback determined correction as discussed here, but also includes a mixing process whereby the particles are allowed to rethermalize. In such a case, many iterations may be used to damp momentum fluctuations for instance. In this demonstration, a measurement and correction are applied but without subsequent state mixing. This is not stochastic cooling, but rather a single iteration of a possible feedback sequence. Instead of damping out the momentum fluctuations of the ensemble, the average momentum of the entire group is damped. A measurement of the velocity distribution is made in order to obtain the center of mass velocity of the ensemble of particles. The information is used in real-time to provide feedback correction to the system in the form of a time dependent optical potential. This potential is a moving 1D optical lattice which traps the atoms and slows them to rest in the laboratory frame.

Coherence and Quantum Optics VIII
Edited by Bigelow et al., Kluwer Academic/Plenum Publishers, 2003

The measurement-correction feedback iteration is done with relatively minor heating of the ensemble.

2 Experimental Setup

Our experiments are performed using cesium atoms from a standard vapor-cell magneto-optic trap (MOT). The MOT apparatus used is described in detail in Ref. [9]. We trap approximately 10^6 cesium atoms with Gaussian distributions in position and momentum with widths of $\sigma_y = 180$ μm and $\sigma_p = 8.5$ $\hbar k$, respectively. Here, $k = 2\pi/\lambda$ is the wavenumber, with wavelength $\lambda = 852$ nm. The experiment starts when the MOT is turned off and the atomic cloud is allowed to fall freely under the influence of gravity for 10 ms, during which it expands to a width $\sigma_y = 350$ μm. After these 10 ms, the cloud is subjected to a velocity measurement through the method of recoil-induced resonances (RIR) [7, 8].

The RIR measurement involves two beams with frequency difference $2\delta\nu$ intersecting in the atomic cloud at angle θ. The beams are both detuned from atomic resonance by Δ_L ($\cong$ 6 GHz in our case). Stimulated Raman transitions between motional states are driven which result in coherent scattering of photons from one beam to the other. The resonance condition [10] for these transitions is

$$2\delta\nu = \frac{2v_y}{\lambda}\sin(\theta/2) \tag{1}$$

where v_y is the velocity in the direction of momentum change between the beams which is vertical in the present work. By choosing a value of $2\delta\nu$, a certain velocity class of the ensemble undergoes stimulated Raman transitions making the scattering rate dependent on the population in the different motional states. Sweeping $2\delta\nu$, therefore, may be used to probe the system's velocity distribution. If done linearly at the appropriate rate, the power in the beams will change in proportion to the derivative of the atomic momentum distribution. This method provides a measure of the velocity distribution but is of limited sensitivity due to mechanical and electrical noise. The sensitivity of this measurement can be greatly enhanced by the application of frequency-modulation (FM) spectroscopy techniques [10].

The experimental setup used is shown in Fig. 1 and is similar to that which is described in Ref. [10]. The two RIR beams start as a single beam generated by a Ti:Sapphire laser which produces approximately 500 mW of light detuned 6 GHz red of the $6S_{\frac{1}{2}}(F = 4) \rightarrow 6P_{\frac{3}{2}}(F' = 5)$ transition near 852 nm. This beam is sent through an acousto-optic modulator (AOM) operating at 80 MHz. This modulator (AOM1) is used to split the original beam into a pair which have a frequency difference of 80 MHz. This pair is to become the pump and probe beams.

The zeroth order beam from AOM1 is double passed through AOM2 operating at 54 MHz+$\delta\nu$ where $\delta\nu$ is a variable frequency. The double pass allows the driving frequency of the AOM to be swept without steering the beam. It is then spatially filtered to clean the beam profile and aligned to hit the atomic cloud after a 10 ms free fall. The beam has a frequency that is shifted 108 MHz+$2\delta\nu$ relative to the original beam, and has a Gaussian intensity profile with a $1/e^2$ waist of 750 μm. This is the pump beam.

The first order beam from AOM1 is double passed through an electro-optic phase modulator (EOM) operating at 28 MHz. The EOM is used to put sidebands on the carrier at $\pm$28MHz . We drive the EOM to produce sidebands 2.5 dB below the carrier. The purpose of double passing the EOM is for reduction of residual amplitude modulation created by the EOM as the birefringence of the lithium niobate crystal drifts in time resulting in polarization modulation of the output beam at the driving frequency. Without compensation, the parasitic change in polarization results in a change

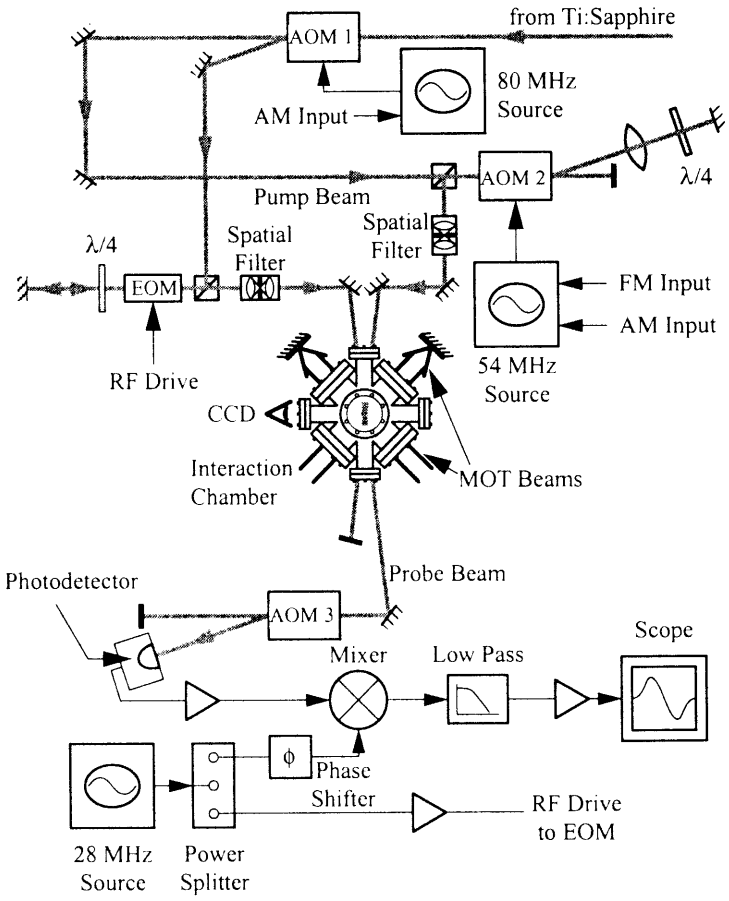

Fig. 1. Experimental setup

in beam amplitude upon passing through the polarizing beam splitter cube that follows the EOM. The double pass setup with the quarter-wave plate allows us to correct for the drifts of EOM birefringence and reduce this effect. Following the EOM double pass, the beam is spatially filtered and aligned to intersect the atomic cloud where it has a $1/e^2$ waist of 750 μm. Since the beam was originally derived as the first order of AOM1, the carrier is 80 MHz above the original Ti:Sapphire beam with sidebands at 53 MHz and 108 MHz. This is the probe beam.

The stimulated Raman transitions between motional states result from the interaction of the pump beam (108 MHz+$2\delta\nu$ relative to the original Ti:sapphire beam) and the upper sideband of the probe beam (at 108 MHz) which intersect at an angle $\theta = 4.5°$. The frequency difference here is $2\delta\nu$, which is experimentally controlled. Depending on the frequency difference, Raman transitions are driven as the resonance condition is met, as in Eq. (1). A frequency difference of $2\delta\nu = 0$ Hz, for example, corresponds to rest in the laboratory frame, whereas $2\delta\nu = \pm 320$ Hz corresponds to velocity classes at $\pm 1\ v_r$, where v_r is the recoil velocity for cesium. For a typical RIR measurement, $\delta\nu$ is linearly swept over a range that includes the entire velocity distribution. The best sweep rate

for an optimal signal depends on the power in the beams as well as the detuning from atomic resonance [10]. Typically, the pump and probe beams have powers of 35 mW and 15 mW, respectively, with $\delta\nu$ swept at a rate of 74.3 MHz/s.

After the beams interact with the atoms, they exit the chamber where the pump beam is blocked. The probe beam passes through AOM3 after which the first order is detected by a photodiode. This additional AOM is used as a fast shutter to protect the photodetector from receiving intensities above the damage threshold during the correction phase which will be described shortly. Prior to interaction with the atoms, the FM sidebands on the probe beam were equal in intensity. The RIR interaction with the atoms results in the scattering of photons from the pump beam into the upper sideband of the probe beam. The imbalance between the FM sidebands results in the amplitude modulation measured by the photodetector. The output of the detector is, therefore, a signal at the sideband frequency (28 MHz) with an amplitude that is proportional to the intensity mismatch between the sidebands (i.e. to the scattering rate that is proportional to the derivative of the velocity distribution).

The output of the photodetector is amplified and mixed with the original 28 MHz signal appropriately phase shifted which is subsequently low-pass filtered to remove the high frequency component and is then amplified. The result is a DC level with the dispersive RIR signal on top of it. The DC level fluctuates to some degree due to fluctuations of the residual amplitude modulation. A typical RIR scan is shown as plot (a) in the timing diagram in Fig. 2.

The RIR measurement determines the average momentum of the cloud of atoms as a zero-crossing of the RIR curve, and this information is used in a feedback scheme to stop the atoms. The intersecting beams create a standing wave or one dimensional lattice that is moving at a velocity of

$$v_{\mathrm{sw}}^{\mathrm{lab}} = 2\delta\nu \frac{\lambda}{2\sin(\theta/2)} \tag{2}$$

with respect to the laboratory and

$$v_{\mathrm{sw}}^{\mathrm{atoms}} = 2\delta\nu \frac{\lambda}{2\sin(\theta/2)} - \frac{\bar{p}}{m} \tag{3}$$

with respect to the atoms. Assuming that the atoms are not initially at rest in the laboratory frame, a linear frequency sweep uniformly decelerates the lattice until it comes to a stop with respect to the atoms. Beyond which, the lattice accelerates in the opposite direction until it comes to a stop in the laboratory frame. The zero crossing of the RIR lineshape corresponds to when the lattice is stationary with respect to the atoms. By turning up the intensity of the beams at the zero crossing, deep potential wells are created that drag the atoms along with them as the standing wave comes to rest in the laboratory frame. This procedure of measurement and correction thereby stops the cloud of atoms in the laboratory frame.

To accomplish this, the RIR signal from the amplifier is fed into an analog electronic trigger circuit. The trigger circuit measures the DC level and subtracts it from the total signal. This leaves only the dispersive RIR lineshape which is compared to a reference voltage level. A trigger signal is generated once the signal passes the threshold level (see plot (a) in Fig.2). Note that the trigger pulse actually comes prior to the zero crossing of the dispersive signal. To compensate for this offset, appropriate delays are added to the electronics that are triggered off this pulse. These delays are typically 20μs and are not visible on the timing diagram in Fig. 2. The output of this comparator trigger is then used to initiate the sequence that stops the atoms. A timing diagram of this sequence is shown in Fig. 2.

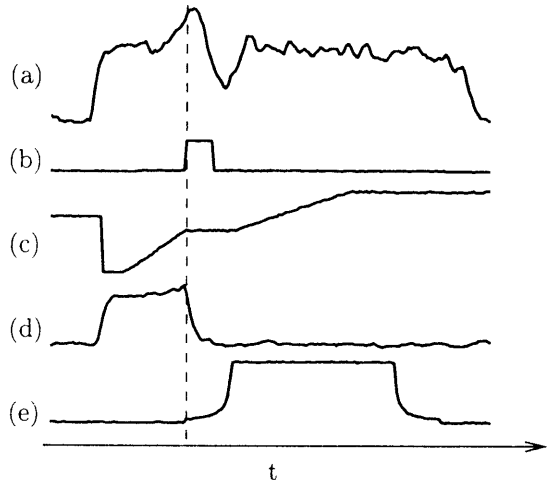

Fig. 2. Timing diagram of voltage signals involved in feedback scheme. The vertical axis is arbitrarily scaled for each signal.

The first curve (a) in Fig. 2 is the untriggered RIR signal shown for reference. It is proportional to the derivative of the momentum distribution. Curve (b) shows the generated trigger pulse, curve (c) shows the linear frequency sweep which changes slope after the trigger for the reason explained below, curve (d) is an RIR signal that was used in a trigger sequence, and curve (e) shows the control signal for the correction which is achieved by increasing the intensity of both RIR beams. The combination of signals (c) and (e) brings the atoms to a stop in the laboratory frame as described above. During the high intensity phase (after the trigger), AOM3 is turned off (via an RF switch) to protect the photodetector. This is seen in curve (d) which is the triggered RIR signal. At the point of trigger on the curve, the light to the photodetector is turned off and the signal vanishes (compare with curve (a)).

The increased intensity of the RIR beams provides the correction. The intensity in each beam increases according to $I(t) = I(0)/(1+\Gamma t)^2$ [11]. This is an adiabatic increase to avoid heating the atoms during this process due to a sudden momentum kick. In the experiment we used $\Gamma = 44.4$ kHz which disturbed the sample very little. Turning on the lattice more quickly was observed to heat the cloud significantly. On the other hand, size constraints limit the amount of time allowed for the adiabatic turn on. The beam size and cloud size are matched for an optimal RIR signal. Therefore, if the intensity is not raised quickly, the atoms will move out of the beam overlap region, and will not be caught in the moving lattice. The initial powers in the pump and probe beams were 35mW and 15mW, and were adiabatically increased to 75mW and 70mW, respectively. Curve (e) in Fig. 2 is the amplitude modulation signal to AOM1 and AOM2 (with different heights for each) that provides this increase to higher intensity.

The frequency sweep is also altered after the trigger pulse. At first, the linear frequency sweep is stopped during the adiabatic turn on. Ideally, the lattice velocity should follow the free fall velocity of the atoms during the adiabatic turn on, but that is difficult due to signal delays (especially due to the low pass filter), therefore we simply hold the lattice at its current speed. Secondly, the acceleration of the lattice after the adiabatic turn-on (proportional to the slope of the frequency) is changed. In an accelerating lattice, atoms will undergo Landau-Zener tunneling [12], escaping the lattice, and will not be stopped. The constant acceleration is decreased to avoid this tunneling, but kept high enough so that atoms would not exit the beam overlap before being stopped. The

initial lattice acceleration for the RIR scan was 810 m/s^2 and was changed to 150 m/s^2 for slowing.

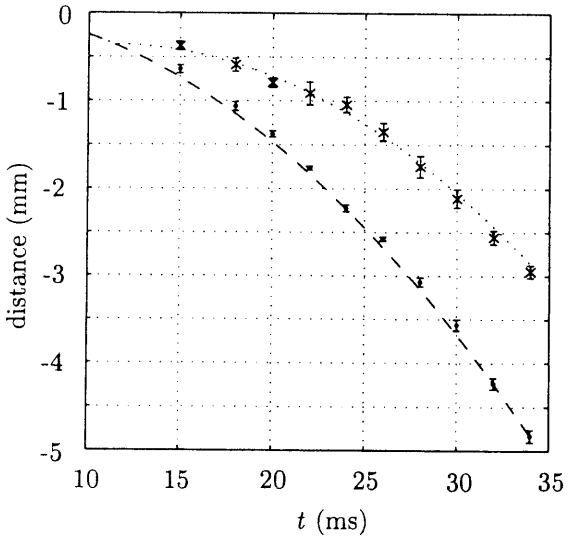

Fig. 3. Center of mass position of a cloud of atomic cesium falling. The data on the lower curve (•) is falling under gravity with no correction. The data on the upper curve (×) is falling with a corrective slow-down at10 ms.

3 Results

The primary result of this experiment is shown in Fig. 3. The data points on the lower curve (•) correspond to the initial cloud of atoms falling under gravity with no corrective slow-down. These are averaged over five free fall sequences. The dashed curve is a ballistic trajectory of the MOT falling under the influence of gravity.

The data points on the upper curve (×) correspond to atoms that were stopped and then allowed to fall again averaged over ten correction sequences. For the first 10 ms, the atoms follow the same free fall curve as described previously. The RIR and slow-down sequence starts at 10 ms after the initial release from the MOT. The sequence stops the falling atoms and then releases them to fall again approximately 1.5 ms later. The dotted curve is a ballistic trajectory with an initial momentum of 0 $\hbar k$ at 11.5 ms. There is good agreement between the data and the idealized trajectory.

Ideally, the trigger pulse turns on the deep well lattice at a time when both the average velocity of the atoms and the lattice are the same. In this case, we achieve stopping efficiency of approximately 80% of the atoms. Perfect stopping efficiency is not possible in our system due to the lower intensities in the wings of the beams creating smaller potential wells that can not slow the atoms. Another source of lower efficiency is noise on the RIR signal which causes the trigger time to vary. This leads to a velocity mismatch between the atoms and the lattice. Typically, the noise causes triggering within a window of 7 recoil velocities about the ideal trigger point. This problem is observed to result in loading efficiencies into the lattice as low as 50%.

To measure the heating effects of this method we plot the width of the cloud σ_y with time in Fig. 4. From this fit, we determine the momentum width in $\sigma_y^2(t) = \sigma_y^2(0) + t^2\sigma_p^2/M^2$. Before the correction sequence the momentum distribution has a width of $\sigma_p = 8.5\ \hbar k$ and after $\sigma_p = 12.2\ \hbar k$.

Heating results from various sources including spontaneous emission and coherent processes involved in the RIR measurement. The beams operate at a detuning of 6 GHz

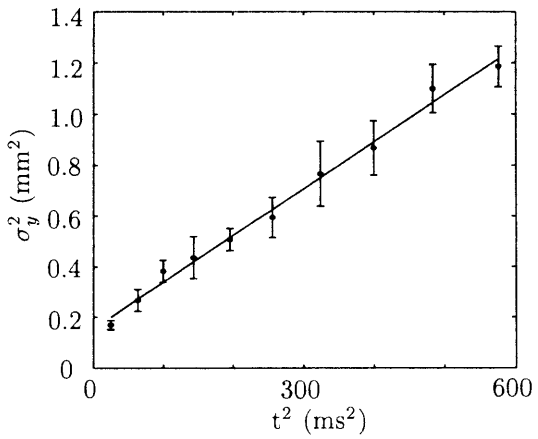

Fig. 4. Temperature measurement of the cloud after stopping showing the cloud's expansion as a function of time.

red from the atomic transition which allows for a reasonably small rate of spontaneous emission. We measure heating to about $\sigma_p = 9\ \hbar k$ from this effect alone. A larger detuning may be used to decrease the spontaneous emission at the expense of a lower well depth for the corrective slow-down.

The RIR measurement is only approximately nondestructive. There is an increase in the momentum width due to the coherent scattering of photons [10]. In our system, the momentum distribution after an RIR measurement when not followed by a corrective slow-down has a width of $\sigma_p = 16\ \hbar k$. In the correction scheme, this heating effect is not fully present since the RIR scan is halted after the trigger which takes place before the halfway point in the scan. The heating effect of the coherent scattering may be reduced by decreasing the scattering rate. This may be accomplished by reducing the power in the beams and/or increasing the detuning. Of course, this is at the expense of the signal for the obvious reason that the signal is smaller if fewer photons are scattered. Fundamentally, the measurement can not be fully nondestructive. Ultimately, the degree of nondestructiveness is determined by the threshold of the RIR measurement, which ideally is dictated by the shot-noise limit.

4 Conclusions

The basic result of this proof-of-principle experiment is that real-time measurement and correction feedback are possible with a controllable amount of perturbation. The center of mass motion of the atoms was controlled in real-time with minimal disturbance to the sample. As demonstrated, this method does not rely on any *a priori* information about atomic motion. As long as the average velocity of the cloud is within the measurement range of the RIR scan, the scheme will work on any unknown average velocity.

5 Acknowledgements

This work was supported by the National Science Foundation, the R. A. Welch Foundation, the U.S.-Israel Binational Foundation, the Sid W. Richardson Foundation, and the Texas Advanced Research Program. T.P.M. acknowledges the support from a National Science Foundation Graduate Research Fellowship. The authors would like to thank B. Gutierrez-Medina, W. H. Oskay, and D. A. Steck for helpful discussions and suggestions.

References and links

1. S. von der Meer "Stochastic Cooling and the Accumulation of Antiprotons," Rev. Mod. Phys. **57**, 689-697 (1985).
2. M. G. Raizen, J. Koga, B. Sundaram, Y. Kishimoto, H. Takuma, and T. Tajima "Stochastic Cooling of Atoms Using Lasers," Phys. Rev. A **58**, 4757-4760 (1998).
3. G. Zhang, J. Shen, J. Dai, and H. Zhang "Cooling Charged Particles in a Paul Trap by Feedback Control," Phys. Rev. A **60**, 704-707 (1999).
4. T. C. Weinacht, J. Ahn, and P. H. Bucksbaum "Controlling the Shape of a Quantum Wavefunction," Nature (London) **397**, 233-235 (1999).
5. J. Ye, D. W. Vernooy, and H. J. Kimble "Trapping of Single Atoms in Cavity QED," Phys. Rev. Lett. **83**. 4987-4990 (1999).
6. N. V. Morrow, S. K. Dutta, and G. Raithel "Feedback Control of Atomic Motion in an Optical Lattice," Submitted for publication (2001).
7. J. Guo, P. R. Berman, B. Dubetsky, and G. Grynberg "Recoil-Induced Resonances in Nonlinear Spectroscopy," Phys. Rev. A **46**, 1426-1437 (1992).
8. J. Guo and P. R. Berman "Recoil-Induced Resonances in Pump-Probe Spectroscopy Including Effects of Level Degeneracy," Phys. Rev. A **47**, 4128-4134 (1993).
9. D. A. Steck, V. Milner, W. H. Oskay, M. G. Raizen "Quantitative Study of Amplitude Noise Effects on Dynamical Localization," Phys. Rev. E **62**, 3461-3475 (2000).
10. M.C. Fischer, A. M. Dudarev, B. Gutierrez-Medina and M. G. Raizen "FM Spectroscopy in Recoil-Induced Resonances," J. Opt. B: Quantum Semiclass. Opt. **3**, 279-287 (2001).
11. A. Kastberg et. al. "Adiabatic Cooling of Cesium to 700nK in an Optical Lattice," Phys. Rev. Lett. **74**, 1542-1545 (1995).
12. C. F. Bharucha, K. W. Madison, P. R. Morrow, S. R. Wilkinson, Bala Sundaram, and M. G. Raizen "Observation of Atomic Tunneling from an Accelerating Optical Potential," Phys. Rev. A **55**, R857-R860 (1997).